6-1-2018

Orbital Characteristics of the Subdwarf-B and F V Star Binary EC 20117-4014 (=V4640 Sgr)

T. Otani
Embry-Riddle Aeronautical University, otanit@erau.edu

T. D. Oswalt
Embry-Riddle Aeronautical University, oswaltt1@erau.edu

A. E. Lynas-Gray
University of Oxford

D. Kilkenny
University of the Western Cape

C. Koen
University of the Western Cape

See next page for additional authors

Scholarly Commons Citation

Authors

T. Otani, T. D. Oswalt, A. E. Lynas-Gray, D. Kilkenny, C. Koen, M. Amaral, and R. Jordan

Publications

6-1-2018

Orbital Characteristics of the Subdwarf-B and F V Star Binary EC 20117-4014 (=V4640 Sgr)

T. Otani
Embry-Riddle Aeronautical University, otanit@erau.edu

T. D. Oswalt
Embry-Riddle Aeronautical University, oswaltt1@erau.edu

A. E. Lynas-Gray
University of Oxford

D. Kilkenny
University of the Western Cape

C. Koen
University of the Western Cape

See next page for additional authors

Scholarly Commons Citation

Otani, T., Oswalt, T. D., Lynas-Gray, A. E., Kilkenny, D., Koen, C., Amaral, M., & Jordan, R. (2018). Orbital Characteristics of the Subdwarf-B and F V Star Binary EC 20117-4014 (=V4640 Sgr). *The Astrophysical Journal, 859*(2). https://doi.org/10.3847/1538-4357/aab9bf

Authors

T. Otani, T. D. Oswalt, A. E. Lynas-Gray, D. Kilkenny, C. Koen, M. Amaral, and R. Jordan

ORBITAL CHARACTERISTICS OF THE SUBDWARF-B AND F V STAR BINARY EC 20117-4014(=V4640 SGR)

T. Otani,[1,2] T. D. Oswalt,[1] A. E. Lynas-Gray,[3] D. Kilkenny,[4] C. Koen,[5] M. Amaral,[6,*] and R. Jordan[7,*]

[1] Department of Physical Sciences and SARA, Embry-Riddle Aeronautical University, 600 S. Clyde Morris Blvd, Daytona Beach, FL 32114, United States

[2] Department of Physics & Space Sciences, Florida Institute of Technology, 150 W University Blvd, Melbourne, FL 32901, United States

[3] Department of Physics, University of Oxford, Oxford, OX1 3RH, United Kingdom

[4] Department of Physics and Astronomy, University of the Western Cape, Bellville 7535, South Africa

[5] Department of Statistics, University of the Western Cape, Bellville 7535, South Africa

[6] Department of Science, Cape Cod Community College, 2240 Iyannough Rd, West Barnstable, MA 02668, United States

[7] Astronomy Department, Whitman College, 345 Boyer Ave, Walla Walla, WA 99362, United States

ABSTRACT

Among the competing evolution theories for subdwarf-B (sdB) stars is the binary evolution scenario. EC 20117-4014 (=V4640 Sgr) is a spectroscopic binary system consisting of a pulsating sdB star and a late F main-sequence companion (O'Donoghue et al. 1997), however the period and the orbit semi-major axes have not been precisely determined. This paper presents orbital characteristics of the EC 20117-4014 binary system using 20 years of photometric data. Periodic Observed minus Calculated (O-C) variations were detected in the two highest amplitude pulsations identified in the EC 20117-4014 power spectrum, indicating the binary system's precise orbital period (P = 792.3 days) and the light-travel time amplitude (A = 468.9 s). This binary shows no significant orbital eccentricity and the upper limit of the eccentricity is 0.025 (using 3σ as an upper limit). This upper limit of the eccentricity is the lowest among all wide sdB binaries with known orbital parameters. This analysis indicated that the sdB is likely to have lost its hydrogen envelope through stable Roche lobe overflow, thus supporting hypotheses for the origin of sdB stars. In addition to those results, the underlying pulsation period change obtained from the photometric data was $\dot{P} = 5.4\,(\pm 0.7) \times 10^{-14}$ d d^{-1}, which shows that the sdB is just before the end of the core helium-burning phase.

Keywords: stars: subdwarfs — stars: binaries — stars: oscillations — stars: evolutions — stars: individual (EC 20117-4014)

Corresponding author: T. Otani
otanit@erau.edu

1. INTRODUCTION

Subdwarf B (sdB) stars are core helium burning objects, found in both the disk and halo of our Galaxy (Saffer et al. 1994). V361 Hya was the first pulsating sdB star to be discovered (Kilkenny et al. 1997) and Østensen et al. (2010) subsequently discovered only twenty new pulsators among the more than 300 sdBs predicted to lie in the V361 Hya instability strip and monitored, suggesting only about 10% of these sdB stars have pulsations detectable from the ground. The sdB observed properties place them in the extreme horizontal branch (EHB) part of the H-R diagram. Their effective temperatures range from 22,000 to 40,000 K and surface gravities range from $5.0 \leq \log g \leq 6.2$ (in cgs units). Their masses are narrowly confined to about $0.5 M_\odot$ (Heber 2009). Subdwarf B stars have experienced mass-loss at the end of the red giant branch phase (Bonanno et al. 2003), in which the hydrogen envelope is lost, leaving a helium core with a very thin inert hydrogen-rich envelope. The loss of the hydrogen envelope prevents the star from ascending the asymptotic giant branch and the star settles on the EHB, spending about 10^8 years as an sdB star. Upon helium depletion in the core they become subdwarf O (sdO) stars burning helium in a shell surrounding a C/O core and, eventually, DAO white dwarfs (Dorman, Rood & O'Connell 1993; Bergeron et al. 1994).

The formation mechanism of sdB stars, i.e. why they lose their hydrogen envelopes, is a matter of current debate. Plausible sdB formation models via binary evolution were constructed by Han et al. (2002, 2003). According to Silvotti et al. (2011), companion stars have been detected in at least 50% of sdB stars, strongly supporting a binary origin. However, some fraction of sdB stars may not be in binaries (Heber 2009; Fontaine et al. 2012). If true, this would require another formation channel, perhaps the single star evolution scenario proposed by Dorman, Rood & O'Connell (1993). Their study of 105 single or wide-binary sdB stars showed that the binary evolution model of Han et al. (2002, 2003) overestimates the number of sdB stars formed through the white dwarf merger channel. In another scenario, the merger of a helium white dwarf with a low-mass hydrogen burning star was proposed as a way of forming single sdB stars (Clausen & Wade 2011). To distinguish between these evolutionary scenarios, orbital information on sdB star binaries is essential.

The existence of sdB pulsators (sdBV) was predicted by Charpinet et al. (1996). Independently, Kilkenny et al. (1997) discovered the first short period sdBV star, EC 14026-2647. These stars are p-mode pulsators, where pulsations are driven by internal pressure fluctuations (Charpinet et al. 2000). The first long period sdBV star, PG 1716+426, is a g-mode pulsator (Green et al. 2003), in which gravity provides the restoring force. Some sdB stars have been discovered to exhibit both p-mode pulsations and g-mode pulsations. These objects are called hybrid pulsators (Schuh et al. 2006; Oreiro et al. 2004).

The pulsation periods of sdBV stars are usually stable (Østensen et al. 2001), and therefore they are good chronometers. A star's position in space may wobble due to the gravitational perturbations of a companion. From an observer's point of view the light from the pulsating star is periodically delayed when it is on the far side of its orbit and advanced on the near side. Changes in the pulse arrival times are detected using the observed-minus-calculated (O-C) diagram. The O-C diagram is a technique that has long been used in the binary star community to search for additional components, orbital period changes, mass loss, etc.

Several planets and substellar companions to sdB host stars have been detected by this method. Silvotti et al. (2007) were the first to detect a planet around the sdB star V391 Peg in this way. Lutz (2011) detected companions to the sdB stars HS 0444+0458 and HS 0702+6043 which appear to be a brown dwarf and an exoplanet, respectively. Mullally et al. (2008) used the O-C method to search for possible planets around DAV white dwarfs. Among the 15 white dwarf stars they surveyed, GD 66 exhibited O-C variations consistent with a $2 M_J$ planet in a 4.5 year orbit. Also, several planets and companion stars to sdB host stars have been detected by the O-C method using eclipse timings. A companion to the sdB star HS 0705+6700 was similarly detected by Qian et al. (2009). While several authors have reported the existence of planets orbiting post-common envelope binaries, these conclusions must be regarded as tentative because they are based on data obtained over a time interval which is the same order as the orbital period proposed for an orbiting planet; further observations over several of the proposed orbital periods would be needed for confirmation. Applegate (1992) proposed an alternative explanation for eclipse timing variations, often referred to as the "Applegate mechanism", as a gravitational coupling of the orbit to changes in the shape of a magnetically active star in the system. Zorotovic & Schreiber (2013) argued for additional observations to distinguish between the Applegate mechanism and planet formation following a common envelope phase. Planets may also survive a common envelope phase of their binary star host, as Kostov et al. (2016) and Veras et al. (2017) discuss. Völschow et al. (2016) concluded that an improved version of the Applegate mechanism, which includes angular momentum exchange between a finite shell and the stellar core, cannot uniquely explain orbital period variations in the sixteen systems they

consider. A further possibility comes from calculations by Chen & Podsiadlowski (2017) which indicate that observed orbital period derivatives in two post-common envelope binaries involving a hot subdwarf (HW Vir and NY Vir) could be produced by a resonant interaction between the binary and a circumbinary disk having a mass in the range $10^{-4} \, \mathrm{M_\odot} - 10^{-2} \, \mathrm{M_\odot}$.

EC 20117-4014 (=V4640 Sgr) is one of the first p-mode sdBV stars to be discovered, and it is known to be a spectroscopic binary system (O'Donoghue et al. 1997). This star was also selected by Otani (2015) as part of a three-year observational search for substellar companions among known sdB pulsators using the O-C method. That project had two goals: (1) determine whether the frequency of detectable companions supports the hypothesis that all, or nearly all, were formed via binary interactions and (2) to examine the frequency with which post main sequence stars in general might harbor "planetary survivors". So far, we have a total of about 20 years of EC 20117-4014 photometric data. In this paper, we present the results of our O-C analysis, and orbital information on the sdB and late F main-sequence companion binary system.

Section 2 provides a summary of the physical properties of EC 20117-4014 and a discussion of the facilities and instrumentation used to obtain the data needed for the O-C analysis. Section 3 outlines our reduction and analysis procedures. Section 4 presents our results derived from the observed pulsation peaks in the frequency spectrum of EC 20117-4014, how they have been used to derive useful constraints on a previously-reported F5 Main Sequence companion. Also, the star's evolutionary phase is discussed. Our conclusions and suggested additional work are summarised in Section 5.

2. TARGET AND OBSERVATIONS

EC 20117-4014 (=V4640 Sgr) is an sdB star originally found in the Edinburgh-Cape (EC) Blue Object Survey (Stobie et al. 1997; Kilkenny et al. 2016). The composite spectra obtained by O'Donoghue et al. (1997) suggested that the sdB component of the EC 20117-4014 binary has a late F main-sequence companion. This companion contributes more than half of the observed flux in the visual band. The apparent magnitude of the system is V = 12.47 ± 0.01, and the magnitude of the sdB star itself is V=13.55 ±0.05 (O'Donoghue et al. 1997). Three pulsation frequencies (7.29 mHz (137.3 s), 7.04 mHz (142.0 s) and 6.35 mHz (157.5 s)) were detected by O'Donoghue et al. (1997), making EC 20117-4014 the fourth member of the class of short period sdBV stars. Further high speed photometry of EC 20117-4014 was obtained and an asteroseismology analysis was performed by Randall et al. (2006), who estimated the effective temperature ($32{,}800 \leq T_{\mathrm{eff}} \leq 36{,}800$ K), the gravity ($5.848 \leq \log g \leq 5.864$), and the mass ($0.50 \leq M_\odot \leq 0.59$). According to Randall et al. (2006), the companion is confirmed to be a late F main-sequence star, but they were unable to set strong constraints on its orbital period. Lynas-Gray (2013) found that the largest pulsation frequency (7.29 mHz) exhibits day-to-day amplitude changes. Other sdBV stars, V541 Hya and KIC 010139564, show similar pulsation amplitude changes that are explained by rotational splitting (Baran et al. 2012; Randall et al. 2009). This suggests the pulsation amplitude changes of EC 20117-4014 may be a consequence of unresolved rotational splitting. The largest pulsation frequency amplitudes in the 2010-2011 data obtained by Otani (2015) showed a linear decrease with time.

The discovery observations of EC 20117-4014 were made with the 0.75-m and 1.0-m telescopes at the Sutherland site of the South African Astronomical Observatory (SAAO) in 1995 (see Table 1 of O'Donoghue et al. (1997)). At that time, both telescopes had (S-11) photomultiplier-based photometers (the response of the system has a similar effective wavelength to the Johnson B, but with a much broader bandpass), though these were replaced by the UCTCCD photometer (e.g. O'Donoghue, Koen & Kilkenny (1996)) in the late 1990s. The UCTCCD could be used on either telescope and our 0.75-m and 1.0-m data post-1996 were obtained with the UCTCCD. Because EC 20117-4014 is relatively bright it was mainly monitored with the SAAO 0.5m telescope between the discovery in 1995 and 2000. The 0.5-m was permanently equipped with a (GaAs) photomultiplier-based photometer until recently decomissioned. For the 0.75-m SAAO telescope observations in 2001 and 2011, UCTCCD was used with a Johnson-B filter. Since 2010, EC 20117-4014 has also been monitored using the SARA-CT 0.6m telescope at the Cerro Tololo InterAmerican Observatory (CTIO) in Chile[1]. Figure 1 provides a finder chart for the target and comparison stars. For the SAAO CCD data, the only comparison star on the CCD chip was GSC07952-01358 (C1 in Table 1). Therefore, this star was used as a comparison star for the SAAO CCD observations. For the SARA-CT observations, we used four comparison

---

[1] The SARA Observatory 0.6-m telescope at Cerro Tololo, Chile, is owned and operated by the Southeastern Association for Research in Astronomy (`saraobservatory.org`).
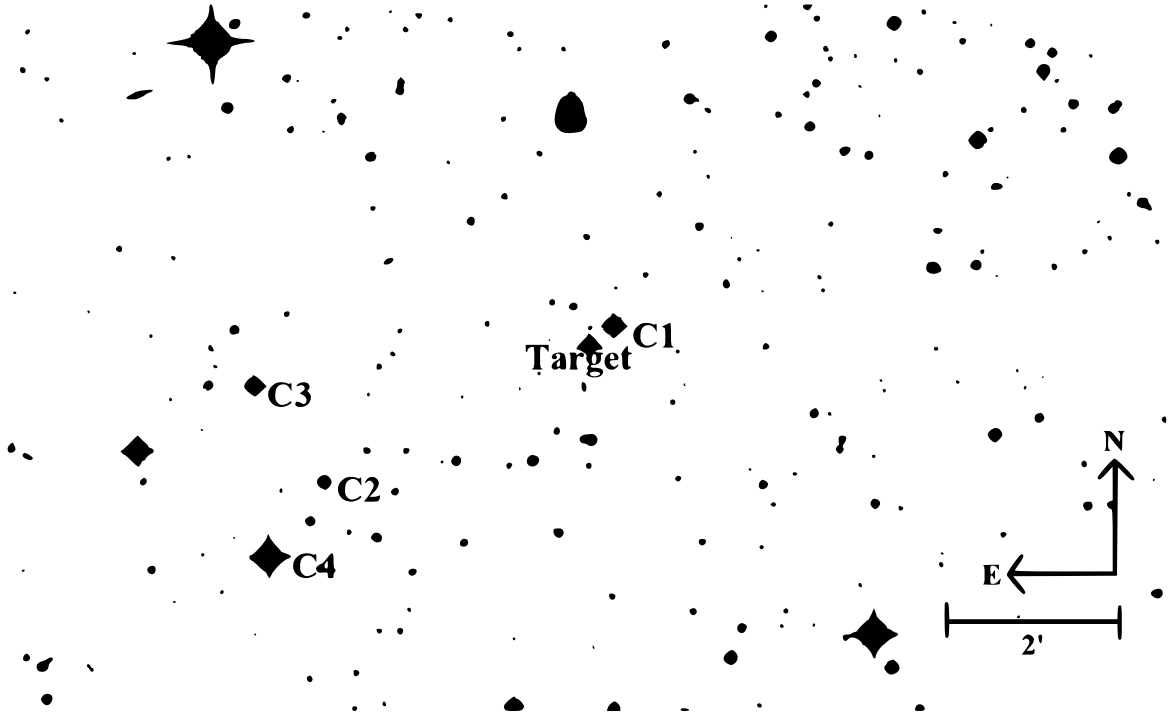
Figure 1. Finder Chart of EC20117-4014 (http://simbad.u-strasbg.fr). The target and the comparison stars (C1-C4) are shown.

Table 1. Coordinates of the Target and Comparison Stars (epoch 2000) (http://simbad.u-strasbg.fr)

Identification Name	RA	DEC
Target	$20^h 15^m 04.^s 79$	-40°05'44.2"
C1	$20^h 15^m 03.^s 23$	-40°05'29.1"
C2	$20^h 15^m 22.^s 20$	-40°07'25.2"
C3	$20^h 15^m 26.^s 68$	-40°06'12.6"
C4	$20^h 15^m 25.^s 91$	-40°08'22.4"

NOTE—For SAAO observations, only C1 (GSC 07952-01358) was used since this is the only comparison star in the field.

stars (including GSC07952-01358). The coordinates of these target and comparison stars are given in Table 1. The observation log is presented in Table 2.

Table 2. Observation Log for EC20117-4014

Date	Start of Run (BJD-2445000)	Length (hr)	Observatory	Publications using the data
1995 May 31	4869.49293	4.4	SAAO	1
1995 Aug 17	4947.23604	8.0	SAAO	1
1995 Aug 18	4948.23415	2.7	SAAO	1
1995 Aug 25	4955.32857	4.1	SAAO	1
1995 Aug 27	4957.25274	5.8	SAAO	1
1995 Sep 19	4980.26625	4.3	SAAO	1
1996 Mar 26	5168.58856	1.4	SAAO	
1996 Apr 21	5194.61163	1.0	SAAO	
1996 Apr 22	5195.60918	1.3	SAAO	
1996 May 26	5229.55177	1.5	SAAO	
1996 May 27	5230.55181	1.5	SAAO	
1996 Jun 28	5262.53746	1.0	SAAO	
1996 Jul 7	5272.48776	1.1	SAAO	
1996 Jul 11	5276.46623	1.1	SAAO	
1996 Jul 16	5281.47772	1.0	SAAO	
1996 Jul 20	5285.45608	1.0	SAAO	
1996 Aug 20	5316.44773	1.1	SAAO	
1996 Aug 21	5317.47060	1.1	SAAO	
1996 Sep 4	5331.41769	1.6	SAAO	
1996 Sep 6	5333.32821	1.1	SAAO	
1996 Sep 8	5335.31267	1.3	SAAO	
1996 Sep 9	5336.37706	1.5	SAAO	
1996 Sep 19	5346.36252	1.5	SAAO	
1996 Sep 20	5347.34214	1.5	SAAO	
1996 Sep 22	5349.34722	1.5	SAAO	
1996 Sep 23	5350.37251	1.4	SAAO	
1996 Oct 12	5369.28318	1.5	SAAO	
1996 Oct 13	5370.26306	1.5	SAAO	
1996 Oct 14	5371.27835	0.8	SAAO	
1996 Oct 27	5384.27263	1.5	SAAO	
1996 Oct 28	5385.26177	1.2	SAAO	
1997 Apr 30	5568.55880	2.6	SAAO	
1997 May 2	5570.57476	2.2	SAAO	
1997 May 4	5572.59402	2.0	SAAO	
1997 May 5	5573.62744	1.1	SAAO	
1997 May 9	5577.59845	1.9	SAAO	

Table 2 *(continued)*

Date	Start of Run (BJD-2445000)	Length (hr)	Observatory	Publications using the data
1997 May 10	5578.63896	1.1	SAAO	
1998 Apr 24	5927.58573	1.8	SAAO	
1998 May 13	5946.57851	1.8	SAAO	
1998 May 31	5964.59448	1.9	SAAO	
1998 Jun 25	5989.57012	2.1	SAAO	
1998 Jul 18	6012.52173	2.1	SAAO	
1998 Jul 19	6014.39887	3.1	SAAO	
1998 Jul 21	6016.41143	2.0	SAAO	
1998 Aug 23	6049.32641	2.0	SAAO	
1998 Aug 24	6050.33752	2.6	SAAO	
1998 Sep 14	6071.31762	2.5	SAAO	
1998 Sep 17	6074.30708	2.2	SAAO	
1998 Sep 18	6075.29670	2.1	SAAO	
1998 Oct 6	6093.29647	2.2	SAAO	
1998 Oct 11	6098.30046	2.3	SAAO	
1999 May 24	6322.60764	1.6	SAAO	
1999 May 26	6324.57515	2.4	SAAO	
1999 Jul 7	6367.48358	2.7	SAAO	
1999 Jul 9	6368.51603	2.3	SAAO	
1999 Aug 8	6399.47168	2.2	SAAO	
1999 Aug 11	6402.41024	2.0	SAAO	
1999 Aug 13	6404.37116	2.1	SAAO	
1999 Aug 15	6406.47675	1.9	SAAO	
1999 Aug 16	6407.50784	1.1	SAAO	
1999 Sep 5	6427.27758	2.2	SAAO	
1999 Sep 17	6439.26778	2.2	SAAO	
1999 Oct 6	6458.26685	2.1	SAAO	
1999 Oct 13	6465.27847	2.2	SAAO	
2001 Jul 12	7103.31649	8.4	SAAO	2
2001 Jul 13	7104.33424	7.9	SAAO	2
2001 Jul 14	7105.30592	8.4	SAAO	2
2010 Oct 14	10483.50415	4.2	SARA-CT	3
2010 Oct 16	10485.55376	3.1	SARA-CT	3
2011 Jun 11	10723.62516	4.0	SARA-CT	3
2011 Jun 12	10724.64718	7.2	SARA-CT	3
2011 Jul 20	10762.62790	4.5	SARA-CT	3

Table 2 *(continued)*

Date	Start of Run (BJD-2445000)	Length (hr)	Observatory	Publications using the data
2011 Jul 21	10763.53925	9.3	SARA-CT	3
2011 Aug 3	10777.25923	4.3	SAAO	4
2011 Aug 6	10780.26951	7.5	SAAO	4
2011 Aug 7	10781.22805	8.5	SAAO	4
2011 Aug 8	10782.20517	9.0	SAAO	4
2011 Aug 9	10783.21753	8.6	SAAO	4
2011 Aug 14	10788.22207	6.3	SAAO	4
2011 Aug 15	10789.20804	8.4	SAAO	4
2011 Aug 16	10790.20824	8.4	SAAO	4
2011 Aug 20	10793.68243	3.8	SARA-CT	3
2011 Aug 21	10794.52048	5.2	SARA-CT	3
2011 Sep 19	10823.48896	5.8	SARA-CT	3
2011 Sep 20	10824.52978	4.8	SARA-CT	3
2011 Sep 21	10825.50645	5.3	SARA-CT	3
2015 Jun 16	12189.69805	5.8	SARA-CT	
2015 Jun 17	12190.71299	4.2	SARA-CT	
2015 Jun 18	12191.69198	6.0	SARA-CT	

References—(1)O'Donoghue et al. 1997; (2) Randall et al. 2006; (3)Otani 2015; (4)Lynas-Gray 2013.

For the 0.6-m SARA-CT observations in 2010, 2011, and 2015, a Bessel-*B* filter was used. The Johnson-B and Bessel-B filters lie close enough in wavelength to have negligible effect on the observed amplitudes of pulsation. The exposure time was 40-s for all runs in this study. For the data obtained in 2015, no filter was used, with an exposure time of 20-s because of a problem with the camera and filter wheel interface. In order to reduce read-out noise, 2×2 pre-binning was used for all images. The pulsations are not expected to be wavelength independent (see Koen (1998)). However, separate analyses were performed using only the data obtained in 1995-2011 and the cumulative data obtained in 1995-2015 in order to compare the results. The O-C analysis results with and without the data obtained in 2015 were the same within the uncertainty level. Therefore, the result including the data observed in 2015 is presented in this paper.

3. DATA REDUCTION AND O-C METHOD

For the SARA-CT data, standard image calibration procedures were performed using the Image Reduction and Analysis Facility (IRAF)[2] to extract the raw intensity values for the target and comparison stars (Tody 1986, 1993). All flat fields were exposed on a twilight sky. For each night's data the aperture that gave the best signal-to-noise ratio (S/N) was chosen and sky annuli were used to subtract the sky background. These values were then divided by similarly extracted intensity values of non-variable comparison stars listed in Table 1. The SAAO photomultiplier data were reduced by removing sky background as a cubic spline fitted to occasional sky measurements and then correcting for atmospheric extinction (see O'Donoghue et al. 1997 for more detail). The SAAO CCD data were reduced using Dophot software (Schechter, Mateo, & Saha 1993) which was modified by Darragh O'Donoghue (see Randall et al. (2006) and Lynas-Gray (2013) for details). For each night, the raw light curves were then normalized to the mean magnitude for that night. A second-order polynomial was used to remove mild curvature in the light curves caused by

---

[2] IRAF is distributed by the National Optical Astronomy Observatories, which is operated by the Association of Universities for Research in Astronomy, Inc. (AURA) under cooperative agreement with the National Science Foundation

differential extinction between the target and comparison stars. All times were corrected to Barycentric Julian Date (BJD). For each night, the raw light curves were then normalized to the mean magnitude for that night.

The normalized light curves were then analyzed using Period04 (Lenz 2004). To improve detection and characterization of the pulsation frequencies and amplitudes, the data were pre-whitened. The pre-whitening technique was originally introduced by (Blackman, & Tukey 1958). After one or more frequencies are identified in the amplitude spectrum, they are removed from each light curve by subtracting the corresponding least-squares fitted sine curve (Sullivan et al. 2008). This analysis was performed for each of the runs listed in Table 2. The data exhibited three pulsation peaks that matched previously published data for EC 20117-4014. Only the two largest pulsations (F1 and F2) were 4σ above the noise background, a threshold commonly used in the variable star community (see Breger et al. 1999). Therefore, only these two pulsations were used in the O-C analysis.

In the O-C method, the "Observed" times of pulsation maxima are compared to "Calculated" times of pulsation maxima, providing a sensitive way to detect period changes of astrophysical phenomena. A good review of the method can be found in Paparo, Szeidl & Mandy (1988).

The O-C will be constant and flat if no period changes are occurring and the assumed period is correct. If the calculated period is constant but incorrect, the O-C will be linear with a positive or negative slope. If the period is changing linearly with time (e.g. due to cooling or magnetic braking), the O-C variations will exhibit a second order polynomial of form $c + bt + at^2$, where $c = \Delta E_0$, $b = \Delta PE$, $a = \frac{1}{2}P\dot{P}E^2$ and t is time. Here E is the integer number of cycles after the first observation, P is the actual period of the pulsation, ΔE_0 is the difference between observed and calculated reference epochs, ΔP is the difference between the actual period and the estimated period (see Winget & Kepler (2008) for details), and $\dot{P} = dP/dt$. The precision of this technique, when applied to observations spanning several years, has allowed empirical measurement of the cooling rates of white dwarf stars and evolution of sdB stars. So far, the $\dot{P}/P$ of sdB stars, V391 Peg, HS 0702+6043, HS 0444+0458 and CS 1246 are observed (Silvotti et al. 2007; Lutz 2011; Barlow et al. 2011).

If the O-C diagram shows periodicities, it is most likely caused by the beating of two closely spaced pulsation frequencies or reflex motion caused by an unseen companion. The beating of two closely spaced frequencies, which may not be resolved in the power spectrum, causes not only sinusoidal variability in O-C using pulsation timings but also sinusoidal variability in pulsation *amplitudes* (Lutz 2011). In this case, the pulsation amplitude variability is 90 degrees out of phase with pulsation timing O-C variability. Therefore O-C sinusoidal variations due to the beating of two closely spaced frequencies are easily distinguished from the O-C periodic variations caused by a companion. Before searching for the sinusoidal signature of a companion in the O-C diagram, a polynomial fit due to the effects of changes in pulsation period were removed. To obtain orbital solutions from O-C diagrams, the O-C and orbital elements relationship of Irwin (1952, 1959) were used. The Levenberg-Marquart (LM) algorithm (Press et al. 1992) was applied to evaluate the parameters of the ephemeris.

To determine "Observed" and "Calculated" maxima, the same method as Silvotti et al. (2007) in detecting the planet V391 Peg b was used. At first, all pulsation periods were determined by Fourier analysis using all data sets. Then the expected pulsation maxima (="Calculated" maxima) were estimated by least squares fitting of a constant period sine curves using all data sets. This equation for the largest pulsation mode (7.29 mHz) is shown below:

$$T = 2445000.0006750 + 0.0015881 \times E \tag{1}$$

On the other hand, "Observed" maxima were determined by least squares fitting of sine curves with the same constant pulsating periods using data for *each* night. Here, all three detected pulsations were used for fitting the data simultaneously. Since all pulsation periods are much shorter than one night, many pulsations occurred on a given night of observation. The time of the maximum of that fit closest to the midpoint of the night of observation was adopted as the "Observed" time of maxima (O) estimated for that night. Because all of a given night's data were used, this procedure maximized the precision to which a given night's phasing could be determined.

The inclination of the orbit with respect to the sky plane, i, is given by the following equation:

$$a_{sdB} \sin i = cT \tag{2}$$

where T is the O-C amplitude, a_{sdB} is the sdB star semimajor axis and c is the speed of light. Thus pulse arrival timing variations can be detected only for the pulsating sdB star, not the companion. The mass function for the system using O-C amplitude, T, is described as:

Table 3. Pulsation Peak Frequencies of EC 20117-4014

Pulsation Mode	Freq	Freq σ	Period	Amplitude	Amp σ
	(mHz)	(mHz)	(s)	(mmag)	(mmag)
F1	7.28484	1.10E-04	137.2	4.3	0.2
F2	7.03529	2.50E-04	142.1	2.0	0.2
F3	6.35145	5.30E-04	157.4	0.9	0.2

$$f = \frac{(M_F \sin i)^3}{(M_{sdB} + M_F)^2} = \frac{4\pi^2 c^3 T^3}{GP^2} \tag{3}$$

where M_F and M_{sdB} are the F and the sdB star masses, P is the orbital period, and G is the gravitational constant.

4. RESULTS AND DISCUSSION

4.1. *Seasonal Pulsation Amplitude Variations*

An example light curve for the night of 2011 September 19 and an amplitude spectrum for the 2011 September 19-21 observing run are displayed in Figures 2 and 3. The highest and the lowest detectable frequencies for the data are 12.5 mHz and 0.10 mHz, respectively. All peaks detected were between 1 mHz and 10 mHz. Three pulsation peaks were found, which are listed in Table 3. To obtain the frequency of the second largest pulsation, the largest pulsation was pre-whitened. To obtain the frequency of the third largest pulsation, the largest and the second largest pulsation were pre-whitened. These peaks matched the previously published results of O'Donoghue et al. (1997) and Randall et al. (2006) within the formal uncertainties. Peaks at 8.35 mHz are distinguished in some of the 1995 and 2001 data, but the S/N ratio was less than 4 σ (this σ is the average Fourier analysis spectrum amplitude after prewriting all three pulsations and this 8.35 mHz signal) and the peak was not detected in other data, so this peak was not included in Table 3. This 8.35 mHz peak is seen only in the data, which is obtained from the SAAO 0.75 m telescope. This frequency is known to be due to the telescope drive of the SAAO 0.75-m telescope in use at the time.

Fig. Set 2. Normalized Light Curves for Each Night

Fig. Set 3. Power Spectra for Each Observation Run

Since seasonal amplitude variations were detected in the largest pulsation frequency by Otani (2015), the possibility of seasonal amplitude changes was investigated. Seasonally-binned pulsation amplitude variations as a function of date are shown in the top panel of Figure 4. These seasonal pulsation amplitude data points are weighted mean amplitudes of each year's data. This weight was obtained from $w = 1/\sigma_i^2$, where σ_i is the pulsation amplitude uncertainty for each night. Triangles represent amplitudes of the largest amplitude pulsation frequency (F1: 7.29 mHz). Diamonds represent amplitudes of the second largest amplitude pulsation frequency (F2: 7.04 mHz), and squares denote amplitudes of the third largest amplitude pulsation frequency (F3: 6.35 mHz). The F2 mode was not detected in the data observed in 2015, and the F3 mode was not detected in the data observed in 2001 and 2015. These seasonal amplitude changes appear to be consistent for all three frequencies, although the F3 variations are comparable with the uncertainties and their reality is questionable. This figure shows that the amplitude of the F1 mode has been decreasing since 2010 at a rate of 0.0021 mmag per day. The pulsation amplitude of the data observed in 2015 is almost one third of the pulsation amplitude of the data observed in 2010. To test whether the changes in amplitudes are correlated, we compared the ratio of the seasonal amplitude of F1 to F2 and to F3. These results are shown in the bottom panel of Figure 4. Both ratios fit zero-slope straight lines within their uncertainties. The weighted average ratios are 0.38 ± 0.03 for F2/F1, and 0.28 ± 0.02 for F3/F1. While the seasonal amplitude variation is consistent in all pulsations, the F1 amplitude decline from 2010 to 2015 (in particular) cannot be understood to be a consequence of rotational splitting. Nonetheless it is of interest to note that Hutchens et al. (2017, their figure 1) observe a similar amplitude decline in the single-mode sdB pulsator CS 1246.

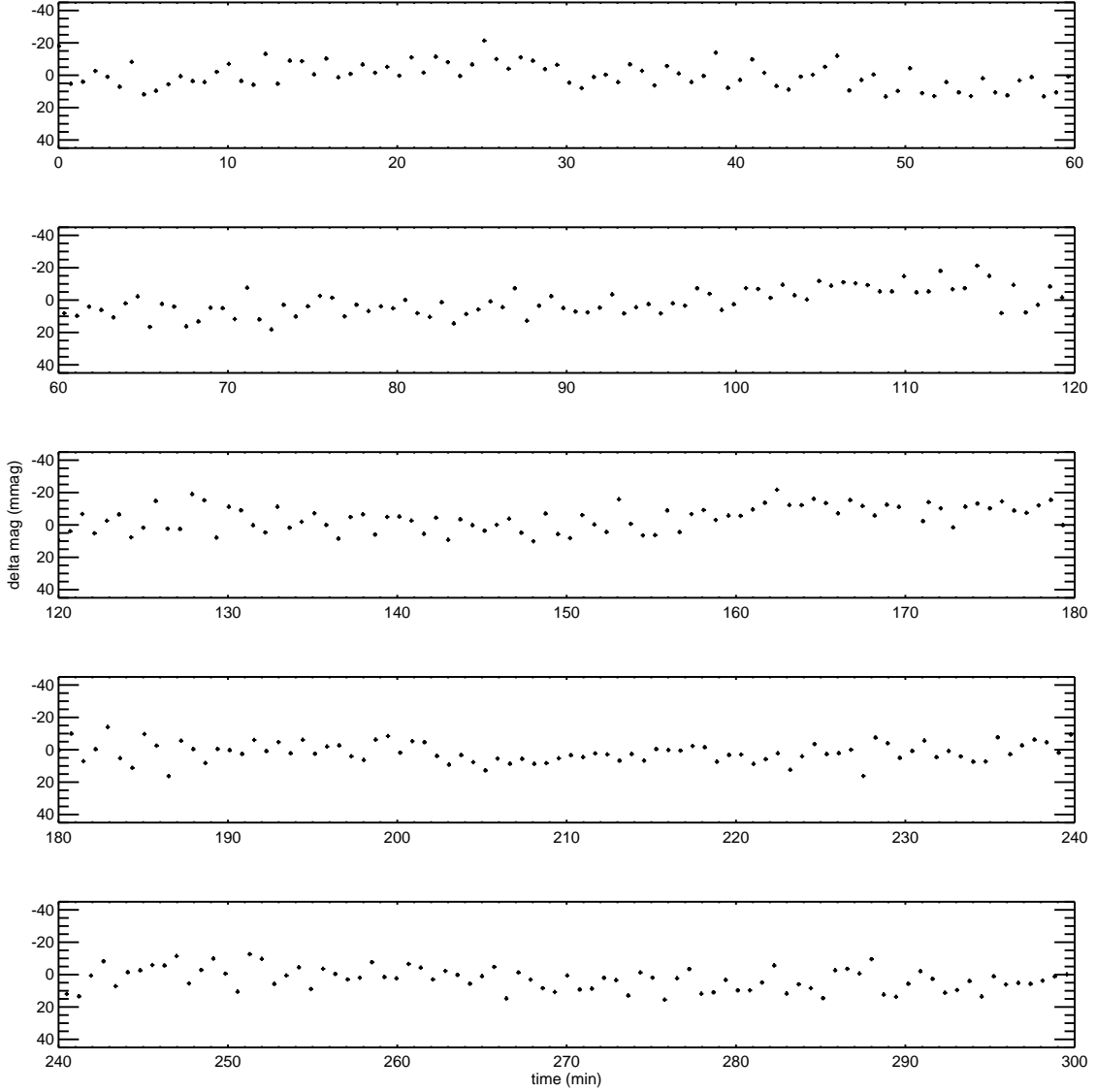### 4.2. *O-C Periodic variation due to the Existence of the Companion*

Figure 2. Example light curve for EC 20117-4014 (2011 September 19). All light curves are available in the Figure Set.

The first and second largest amplitude pulsations F1 and F2 were used for an O-C analysis. The S/N ratios of the third largest pulsations (F3) for each night were less than $4\,\sigma$, so this mode was not used in our analysis. Two distinct causes of period variation were identified in both F1 and F2 (O-C) values. In addition to the near sinusoidal variation due to light travel-time changes caused by the reflex motion of the pulsating sdB star, a second order polynomial variation attributable to sdB star evolution was also discernible. Orbital and evolution contributions were fitted simultaneously; in fitting orbits, a single offset was established so as to minimize the difference between the F1 and F2 orbits. The pulsation period change is $\dot{P} = 5.4\ (\pm\ 0.7) \times 10^{-14}$ d d^{-1}. The removed second order polynomial curves for O-C diagrams is:

$$O - C = (2.6(\pm 0.4) \times 10^{-6})t^2 - (4.0(\pm 0.6) \times 10^{-2})t + 1.5(\pm 0.2) \times 10^2 \tag{4}$$

Here, t is BJD - 2445000.

The rate of period change ($\dot{P}$) indicates the age of the sdB star after the zero-age extreme horizontal branch (ZAEHB) (Charpinet et al. 2002). For p-modes, $\dot{P}$ is positive during the first evolutionary phase, which is before the thermonuclear fuel in its center is exhausted. $\dot{P}$ is negative during the second evolutionary phase, which is after the
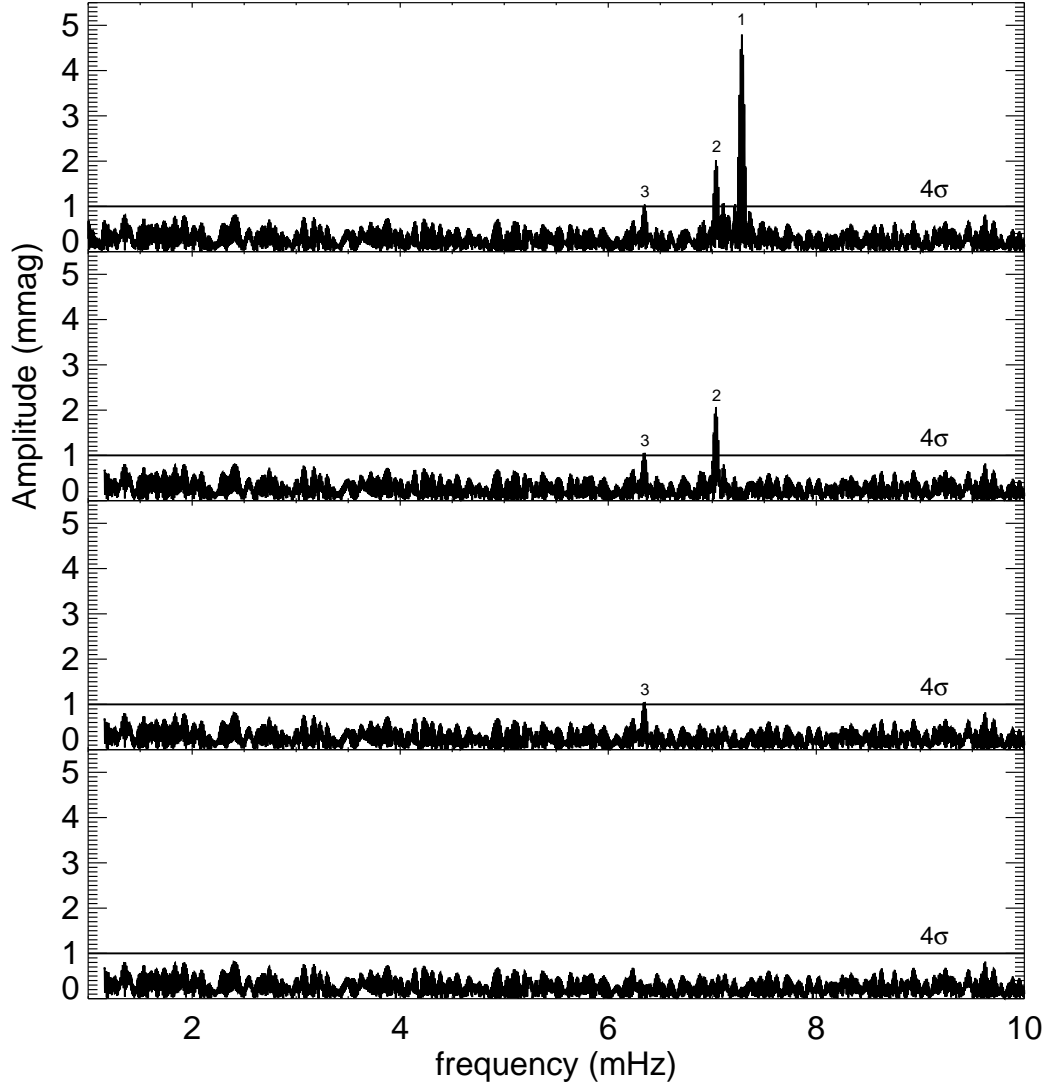
Figure 3. Example Fourier analysis for EC 20117-4014 (2011 September 19-21). The top panel shows the three most significant pulsation peaks (indicated by numbers) and the four-sigma threshold for significance adopted here. The lower panels show the successive steps of pre-whitening by sequentially removing the next largest pulsation peaks. The bottom panel shows the residual after all three pulsation peaks have been removed. In each panel, horizontal lines indicate 4σ noise levels. Fourier transform of each observing night data are available in the Figure Set.

depletion of thermonuclear fuel in its center and before the post-EHB evolution. The change of sign occurs around 87-91 Myr after the ZAEHB. The positive values of $\dot{P}$ for EC 20117-4014 (sdB) denote that the the star is still in the first evolutionary phase. The age of EC 20117-4014 (sdB) can also be estimated from its effective temperature and surface gravity g. Figure 1 of Fontaine et al. (2012) indicates that the age of EC 20117-4014 (sdB) is 90 ± 5 Myr. Therefore the sdB component of EC 20117-4014 is about to end its core helium-burning phase.

Also, we can set an upper limit on the age of the sdB star since the zero-age main sequence (ZAMS). Choi et al. (2016) suggests that the Main Sequence (MS) lifetime of a 1.5 $M_\odot$ star, like the late F main-sequence companion, is about 2.5 Gyr (See Figure 12 of their article). Assuming that both the sdB star and its F companion are coeval, an upper limit to the age of the sdB star is therefore 2.5 Gyr. However, this argument is not valid if large mass exchange from sdB progenitor to the companion occured during the RLOF evolution.

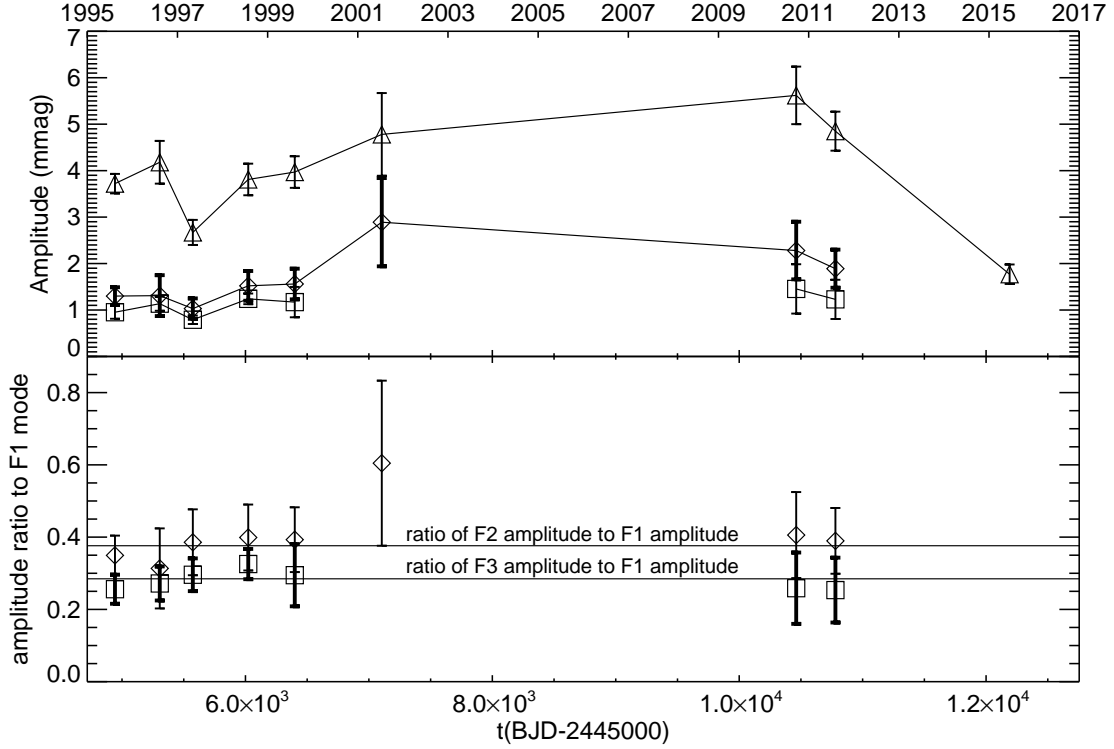The time scale for radius change is also obtained from the time scale for period change:

Figure 4. EC 20117-4014 seasonal pulsation amplitude variations of each pulsation mode (top) and pulsation amplitude ratios of the second and third largest pulsation modes compared with the largest amplitude pulsation mode of 7.29mHz (bottom). *Top* : Data points of the largest amplitude pulsation mode F1: 7.29 mHz are marked by triangles. The points of the second and third largest amplitude pulsation modes, F2 (7.04 mHz) and F3 (6.35 mHz), are marked by diamonds and squares, respectively. Each data point is the weighted average amplitude during each year (1995, 1996, 1997, 1999, 2001, 2010, 2011, and 2015). The F2 mode was not detected in the data observed in 2015, and the F3 mode was not detected in the data observed in 2001 and 2015. The F1 mode and F2 modes show obvious pulsation amplitude variations. Seasonal amplitude variations appear to be consistent for all three frequencies, although F3 mode amplitude variations are too small (compared to the uncertainty) to confirm the variations are real. *Bottom* : F2 mode (diamonds) and F3 mode (squares) pulsation amplitudes compared to F1 amplitudes. Both ratios fit straight lines. The horizontal lines are the weighted average ratios of both frequencies, which is 0.38 ± 0.03 for amplitude ratios F2/F1, and 0.28 ± 0.02 for F3/F2.

$$\frac{\dot{P}}{P} \approx \frac{3}{2}\frac{\dot{R}}{R} \tag{5}$$

Here, R is the radius of the star. For EC 20117-4014, the time scale for period change $(P/\dot{P})$ is roughly 8.0×10^7 yr. This value corresponds to a time scale for the radius increase of $R/\dot{R} \approx 1.2 \times 10^8$ yr. According to Figure 3 of (Kawaler 2010), $R/\dot{R} \approx 2 \times 10^8$ yr at the first phase of core helium burning and it will turn negative at the second phase of shell burning. $R/\dot{R}$ for the sdB component of EC 20117-4014 is about a half of 2×10^8 yr, and this also indicates that this star's core-burning is about to terminate.

Figure 5 presents the phase-folded O-C diagrams for F1 and F2 after the removal of polynomials given by equation (4). For F2, the only nights shown are those for which the pulsation amplitude is 4-σ above the noise level. The pulsation periods used are 137.2729-s for F1 and 142.1477-s for F2. Table 4 lists all O-C data points for F1 and F2 pulsation modes respectively. The solid curves in Figure 5 are the best fitting orbital solutions. The orbital periods are 792.3 ± 0.3 d, and these are the same within the uncertainties. Initially, we inadvertently omitted 1998 data from the (O-C) diagram. When the 1998 data were included, these fitted the already established O-C curve well. The best fitted orbital solutions for F1 and F2 O-C data points are shown in Table 5. The formal χ^2 values are 86.5 (F1) and 27.4 (F2), respectively. Degrees of freedom of F1 and F2 are 84 and 30. The corresponding right tail p-values are 0.40 and 0.60. Therefore, the correlation between the periodicity of the O-C data points and the binary motion with P=792.3 days are not rejected. The chi-squared values being consistent with the number of degrees of freedom suggest
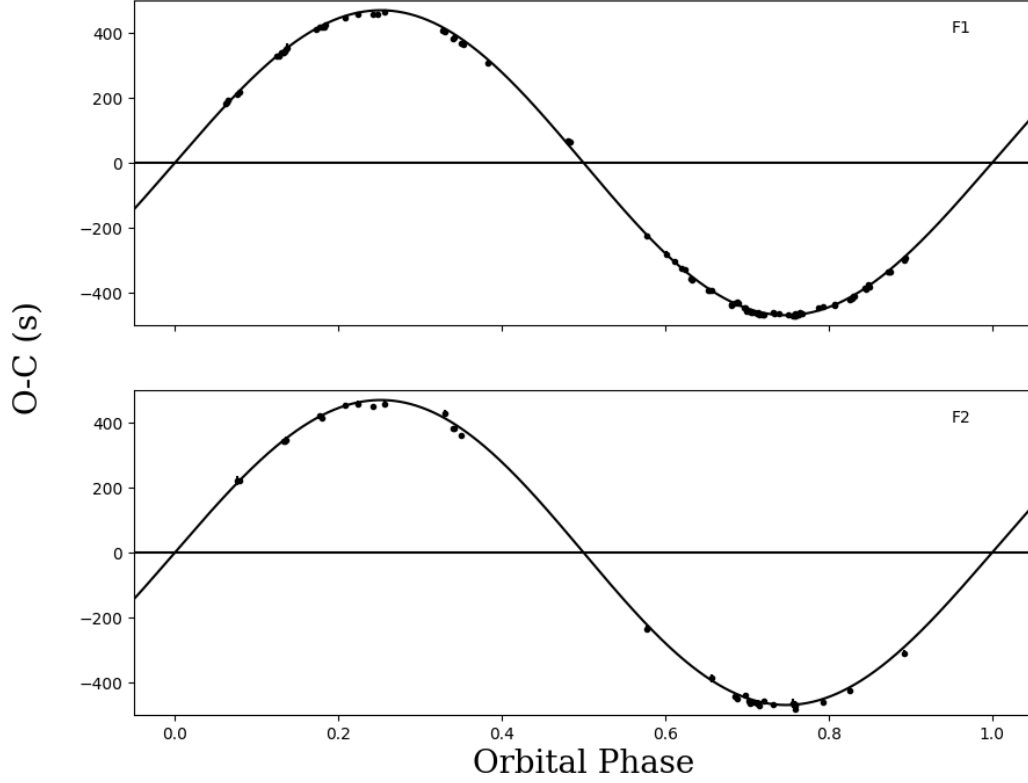
Figure 5. Phase-folded O-C curves for EC 20117-4014 constructed from the largest and the second largest amplitude pulsations (F1: 7.29 mHz at the top and F2: 7.04 mHz at the bottom). The third largest amplitude pulsation of each night was lower than $4\,\sigma$ above the noise level so it was not used for the O-C analysis. Each square represents the O-C value of each entire night. O-C uncertainties of some data points are smaller than the symbol size. Periods and amplitudes of fitted curve is 792.3 d and 468.9 s.

that all relevant physical information has been extracted from the data; in particular, there is no evidence for a third body associated with the EC 20117-4014 binary which would not have been accounted for in our model.

Table 4. O-C data points for F1 (7.29 mHz) and F2 (7.04 mHz) pulsation modes before removing the second order polynomial fit

Time	[F1]O-C	[F1] O-C uncertainties	[F2]O-C	[F2] O-C uncertainties
(BJD-2445000)	(s)	(s)	(s)	(s)
4869.492986	470.0	2.0	472.0	5.5
4947.402781	396.7	1.9	402.7	4.9
4948.291201	397.5	2.9	402.0	8.9
4955.328631	381.2	2.7	381.8	6.7
4957.252794	376.9	2.3		

Table 4 continued on next page

Table 4 *(continued)*

Time	[F1]O-C	[F1] O-C uncertainties	[F2]O-C	[F2] O-C uncertainties
(BJD-2445000)	(s)	(s)	(s)	(s)
4980.266303	319.2	4.6		
5168.588619	-315.1	3.6		
5194.611691	-383.6	5.6		
5195.609237	-381.7	4.6		
5229.582828	-438.1	5.2		
5230.582731	-435.7	4.5	-426.2	10.6
5262.537515	-457.3	7.0		
5272.487817	-460.3	6.9		
5276.466287	-462.0	5.6	-451.1	18.5
5281.489239	-457.9	5.5		
5285.456137	-454.3	4.8		
5316.471197	-432.4	5.0		
5317.494223	-427.2	6.3		
5331.450016	-412.3	5.6	-415.5	14.9
5333.350491	-409.7	8.1		
5335.340110	-404.4	4.5		
5336.408112	-402.8	7.3		
5346.393672	-378.5	5.7		
5347.373323	-383.0	5.8		
5349.378340	-366.6	7.1		
5350.400659	-375.8	7.6		
5369.315228	-329.4	4.4		
5370.294472	-326.8	6.3		
5371.294833	-330.3	5.4		
5384.303378	-291.9	8.0	-302.2	11.7
5385.286270	-287.2	4.6		
5568.558797	332.6	3.1		
5570.574757	334.5	4.7		
5572.594017	343.5	7.5		
5573.627437	342.5	5.6		
5576.640367	354.5	3.5		
5577.598447	354.2	3.7	351.8	12.1
5578.638957	358.3	14.2		
5927.623752	-223.2	4.3	-233.5	13.4
5946.615308	-282.1	11.0		
5954.636558	-302.7	3.7		

Table 4 continued on next page

Table 4 (continued)

Time	[F1]O-C	[F1] O-C uncertainties	[F2]O-C	[F2] O-C uncertainties
(BJD-2445000)	(s)	(s)	(s)	(s)
5964.633991	-326.6	4.0		
5989.612737	-391.4	4.1	-385.8	12.4
6012.564885	-430.5	4.2	-443.5	8.4
6014.466184	-429.7	3.6	-449.9	9.1
6016.453894	-433.5	4.2		
6049.365569	-462.3	6.4	-466.5	11.5
6050.390923	-464.1	3.0		
6071.370080	-464.4	3.1	-466.8	7.9
6074.351007	-466.9	3.9		
6075.339904	-462.8	3.9		
6093.341990	-447.1	6.4		
6098.348228	-444.6	3.5	-459.3	9.6
6322.602836	206.6	4.7	219.0	13.3
6324.570313	214.2	3.5	218.9	6.0
6367.457465	337.4	3.6	342.1	6.9
6368.507951	341.1	3.1	340.2	10.1
6399.464757	407.8	4.3		
6402.403646	415.7	4.0	420.2	9.3
6404.364641	415.0	3.6	412.1	8.1
6406.470197	413.9	4.4		
6407.501447	420.4	7.3		
6427.272280	443.8	5.0	450.8	9.9
6439.263252	453.4	3.8	456.6	10.8
6458.263947	454.5	4.1		
6465.276215	459.9	3.2	456.4	10.6
7103.488750	173.9	9.4		
7104.488620	177.6	6.1		
7105.474873	186.2	6.3		
10483.589470	417.7	5.7		
10485.617570	415.3	6.0	423.4	13.2
10723.804710	-342.7	7.0		
10724.797720	-347.6	4.8		
10762.721360	-420.4	7.6		
10763.733280	-423.9	4.6		
10777.350960	-441.2	3.7		
10780.428190	-443.8	2.5	-440.3	5.4

Table 4 *(continued)*

Time	[F1]O-C	[F1] O-C uncertainties	[F2]O-C	[F2] O-C uncertainties
(BJD-2445000)	(s)	(s)	(s)	(s)
10781.391280	-444.0	4.1	-450.6	8.4
10782.395440	-445.4	3.0	-444.7	8.5
10783.396050	-444.4	2.9	-445.6	9.0
10788.339390	-448.9	3.3	-448.5	16.1
10789.383570	-447.5	3.0	-447.5	8.2
10790.383670	-451.5	2.3	-455.8	6.6
10793.761090	-451.5	5.6		
10794.629430	-452.3	3.6	-442.2	8.8
10823.610400	-454.1	4.0	-450.6	8.2
10824.618790	-454.9	4.4	-454.2	9.2
10825.615890	-456.4	3.6	-464.2	11.4
12189.819940	108.8	4.8		
12190.800550	106.1	5.8		
12191.817640	104.6	5.4		

Note—Time is mid-observing time.

The resulting period of a periodic curve (P= 792.3 d) does not match sinusoidal variabilities in the F1 and F2 pulsation amplitudes, so these are not due to the beating of two closely spaced pulsation frequencies. Therefore, we concluded that the resulting variations are due to the light-travel effects caused by the F-type companion.

Most subdwarf-B (sdB) stars in binary systems have companions which are white dwarfs or M-dwarf Main Sequence stars (Kupfer et al. 2015); these have short orbital periods ($\lesssim$ 10 days) and are understood (Han et al. 2002, 2003; Xiong et al. 2017) to be a consequence of evolution in a common envelope. A few sdB binaries have longer orbital periods with a F- or G-type giant or Main Sequence star; EC 20117 − 4014 was confirmed in the present paper to be an example and Aznar Cuadrado & Jeffery (2002), Németh et al. (2012) and Vos et al. (2017) discovered some additional systems. SdB stars in wide binaries are formed (Han et al. 2002, 2003) as a consequence of a red giant progenitor losing almost all of its hydrogen envelope, at the onset of core helium-burning, through stable Roche lobe overflow (RLOF); their calculations suggest that the orbits should be circular and have periods $\lesssim$ 500 days.

Orbital element determination for long-period sdB binaries presents a greater challenge than for those with short periods. Radial velocity observations by Østensen & Van Winckel (2012); Deca et al. (2012); Barlow et al. (2013); Wade et al. (2014), identified sdB stars having a main sequence or giant companion with orbital periods > 500 days, significantly greater than the Han et al. (2002, 2003) orbital-period distribution would suggest. Chen et al. (2013) reproduce the orbital-period distribution Østensen & Van Winckel (2012) observe using detailed binary evolution calculations for the stable RLOF channel, improving on the simplified binary population synthesis by Han et al. (2003). The estimated period of binaries that went through this RLOF channel is P = 400 - 1100 d. The derived orbital period of the EC 20117-4014 binary system (P = 792.3 d) falls in the middle of this range.

Figure 6 shows the residuals of the fitted orbital solution of O-C data points shown in Figure 5. Vos et al. (2015, their figure 1) plot orbital eccentricities against periods for those long-period sdB binaries for which orbital elements had been determined at the time of publication. A clear correlation is apparent with longer period systems having higher orbital eccentricities. Modifications to the binary module of the stellar evolution code Modules for Experiments in Stellar Astrophysics (Paxton et al. 2011, 2013, 2015, MESA) by Vos et al. (2015), to include eccentricity pumping processes, results in binary systems with observed orbital eccentricities when eccentricity pumping via a circumbinary disk is accompanied by phase-dependent RLOF. A remaining difficulty is the model prediction of some high orbital eccentricities for short periods which are at variance with available observations.
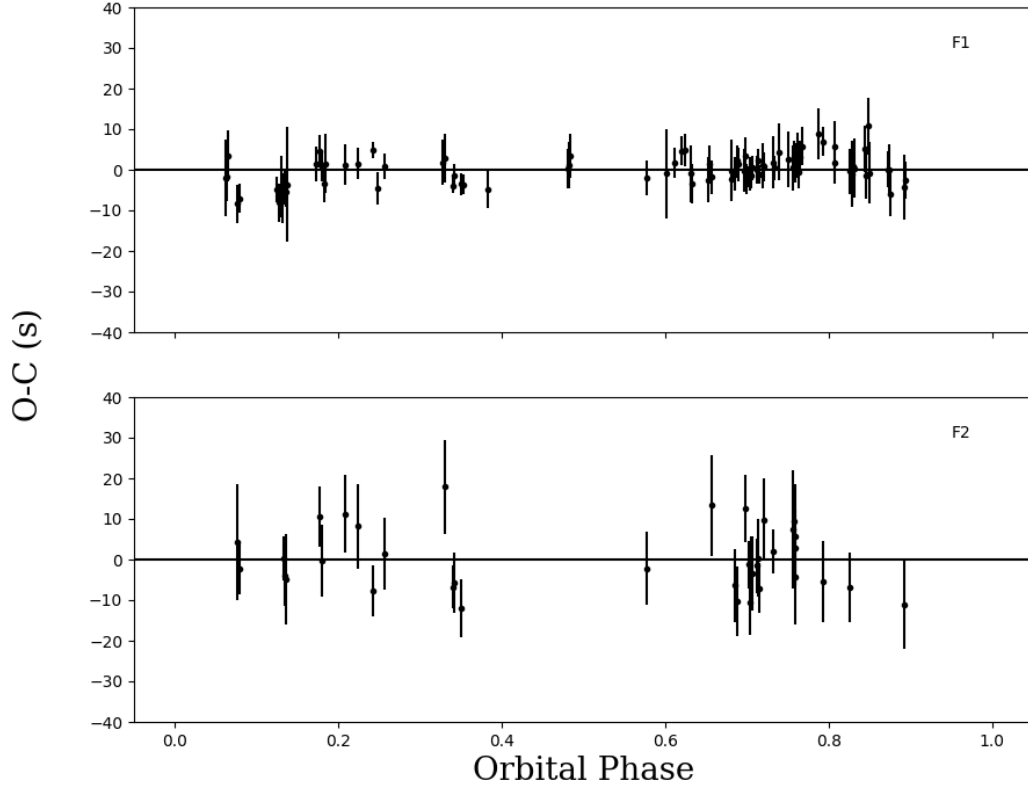
Figure 6. Residuals of the fitting of O-C data points shown in Figure 5. The top panel show the residual for F1 O-C data points and the bottom panel show the residual for F2 O-C data points.

The deduced period of 792.3 days suggested an orbital eccentricity of 0 - 0.07 on the basis of the Vos et al. (2015) figure 1. No significant eccentricity is detected in the EC 20117-4014 binary system, and the upper limit to the eccentricity is 0.025 if 3σ is used as an upper limit. The eccentricity of this binary system has the lowest upper limit among all wide sdB binaries with known orbital parameters (Vos et al. 2017).

Using the periodicity shown in Figure 5 (792.3 ± 0.3 d), which is due to the orbital motion, the semi-major axis for the star's orbit was calculated. If both the sdB star mass (m_{sdB}) and F star mass(m_F) are known, semi-major axes of both sdB and F main sequence stars are calculated using Equations (2) and (3). According to Randall et al. (2006), the EC20117-4014 sdB star mass range is $m_{sdB} = 0.50 - 0.59 M_\odot$. However, the F star mass of the EC 20117-4014 system is unknown. Therefore, the F stars' mass was estimated from the stellar type. Since the estimated stellar type of this companion is F5V or late F main-sequence (O'Donoghue et al. 1997), the main-sequence mass range (Schmidt-Kaler 1982) of F5-G0 (which is 1.40-1.05 $M_\odot$) was used to estimate the semi-major axis. The semi-major axes ranges of the sdB star and the F main sequence star are $a_{sdB} = 1.3$-1.5 AU and $a_F = 0.5$-0.7 AU. The inclination was computed using possible mass ranges. The inclination range obtained is $i = 37.9°$- 48.0°. It is not surprising that eclipses have not been detected in the observed light curves. The orbital parameters are shown in Table 5.

In principle, the F main sequence companion should be detectable via radial velocity variations. However, radial velocities are difficult to measure for sdB stars because of their high gravity (which broadens the line profiles). Generally, the (non-relativistic) radial velocity of the sdB star can be estimated using the mass function:

$$f = \frac{(M_F \sin i)^3}{(M_{sdB} + M_F)^2} = \frac{PK^3}{2\pi G} \tag{6}$$

Table 5. Orbital information of the EC 20117-4014 system

Parameters	values
Period (days)	792.3 ± 0.3
Amplitude (s)	468.9 ± 1.1
eccentricity	$0.004 \pm^{0.007}_{0.004}$
zero point of time (BJD-2445000)	4673.0 ± 0.4
radial velocity for sdB star K_{sdB} (km/s)	12.90 ± 0.03
semimajor axis a_{sdB} (AU)	1.3 - 1.5
semimajor axis a_{F5} (AU)	0.5 - 0.7
inclination (degrees)	37.9 - 48.0

NOTE—semimajor axes a_F & a_{sdB} and inclination i are estimated ranges using possible sdB and F main sequence stars masses.

where M_{sdB} and M_F are the masses of the sdB star and F companion. P, K, and G are the orbital period, radial velocity semi-amplitude, and gravitational constant, respectively. Comparing this mass function with the previously obtained mass function using O-C amplitude, T, (see equation (2)), the relationship between K and T is described as:

$$K = \frac{2Tc\pi}{P} \tag{7}$$

This equation only depends on T and P, and is not dependent on M_{sdB} and M_F. Using this equation yields an estimate for the sdB star radial velocity amplitude of 12.90 ± 0.03 km s^{-1}.

Silvotti et al. (2014) succeeded in measuring the radial velocities of sdB stars to a precision of 50-100 m s^{-1} (5-sigma level) using the 3.6 m *Telescopio Nazionale Galileo* (TNG). The EC 20117-4014 sdB star radial velocity amplitude obtained is much larger than this, so it is possible to confirm the companion using the radial velocity method. However, as shown here, much smaller telescopes (1-m class) are adequate to detect it using the O-C method.

5. CONCLUSIONS

This paper presents an orbital solution for the EC 20117-4014 binary and the evolutionary stage of its sdB component. The formation theory for sdB stars is still hotly debated and the frequency with which companions are found may help settle this issue. In particular, orbital element determination for long-period sdB + F/G dwarf binaries is not as common as those with short periods, and only 12 binaries' orbital solutions were obtained so far. Among those systems, EC 20117−4014 is unique in that the orbital elements were obtained using the changing light travel time across the sdB star orbit, not using radial velocities. Photometric data of EC20117-4014 for 20 years shows obvious periodic variations in both the largest and the second largest amplitude pulsation frequencies and allowed an orbital solution for the F main-sequence companion and the sdB star. The data indicate the orbital parameters of the binary system are:

1. Orbital period P = 792.3 ± 0.2 days

2. The upper limit of the eccentricity is 0.025. This is the lowest upper limit of the eccentricity among all 12 wide sdB binaries with known orbital parameters.

3. The light-travel time amplitude A = 468.9 ± 1.1 s

4. Inclination $i = 37.9° − 48.0°$, which does not permit eclipses.

Importantly, the EC 20117-4014 sdB star represents another example of a system that has very likely experienced binary evolution, and lost almost all of its hydrogen envelope through stable RLOF. The 20 years of photometric data also showed the time scale for period changes $\dot{P}/P$. The $\dot{P}/P$ and the corresponding time scale for radius increase indicates that the EC 20117-4014 is about to deplete thermonuclear fuel in its center.

Facilities: SAAO: 0.5m, SAAO: 0.75m, SAAO: 1.0m, CTIO:0.6 m

Software: Period04 (Lenz 2004)

REFERENCES

Aznar Cuadrado, R. & Jeffery, C. S., 2002, AAS Meeting Abstracts, 385, 131

Applegate, J. H. 1992, ApJ, 385, 621

Barlow, B. N., Dunlap, B. H., Clemens, J. C., Reichart, D. E., Ivarsen, K. M., LaCluyze, A. P., Haislip, J. B., & Nysewander, M. C., 2003, A&A, 398, 283

Barlow, B. N., Liss, S. E., Wade, R. A., & Green, E. M., 2012, ApJ, 771, 23

Baran, A. S., Reed, M. D., Stello, D., et al. 2012, MNRAS, 424, 2686

Bonanno, A., Catalano, S., Frasca, A., Mignemi, G., & Paternò, L., 2003, A&A, 398, 283

Bergeron, P., Wesemael, F., Beauchamp, A., Wood, M. A., Lamontagne, R., Fontaine, G., & Liebert, James, 1994, ApJ, 432, 305

Breger M. et al., 1999, A&A, 349, 225

Blackman, R. B. & Tukey, J. W., 1958, Bell Syst. Tech. J., 398, 283

Charpinet, S., Fontaint, G., Brassard, P., & Dorman, B., 1996, ApJL, 471, L103

Charpinet, S., Fontaine, G., Brassard, P., & Dorman, B., 2000, ApJS, 131, 223

Charpinet, S., Fontaint, G., Brassard, P., & Dorman, B., 2002, Ap&SS, 140, 469

Chen, X., Han, Z., Deca, J., & Podsiadlowski, P. 2013, MNRAS, 434,186

Chen, W.-C., & Podsiadlowski, Ph. 2017, ApJL, 837, L19

Choi, J., Dotter, A., Conroy, C., Cantiello, M., Paxton, B., & Johnson, B. D., 2016, ApJ, 823, 2

Clausen, D., & Wade, R. A., 2011, ApJ, 733, L42

Deca, J., Marsh, T. R., & Østensen, R. H. et al., MNRAS, 421, 2798

Dorman, B., Rood, R. T., & O'Connell, R. W., 1993, ApJ, 419, 596

Efron, B., 1979, Ann. Statist, 7, 1, 1-26

Fontaine, G., Brassard, P., Charpinet, S., Green, E. M., Randall, S. K., & Van Grootel, V., 2012, A&A, 539, 12

Green, E. M. et al., 2003, ApJ, 583, 31

Han, Z., Podsiadlowski, Ph., Maxted, P. F. L., Marsh, T. R., & Ivanova, N., 2002, MNRAS, 336, 449

Han, Z., Podsiadlowski, Ph., Maxted, P. F. L., & Marsh, T. R., 2003, MNRAS, 341, 669

Heber, U., 2009, ARA&A, 47, 211

Hinkley, D., 1988, J. Royal Stat. Soc. Series B, 50, 3, 321

Hutchens, Z. L., Barlow, B. N., Vasquez, S. A., Reichart, D. E., Haislip, J. B., Kouprianov V. V., Linder, T. R. & Moore, J. P., 2017, Open Astronomy, 26, 252

Irwin, J. B., 1952, ApJ, 116, 211

Irwin, J. B., 1959, AJ, 64, 149

Kawaler, S. D., 2010, AN, 331, 1020

Kilkenny, D., O'Donoghue, D., Koen, C., Stobie, R. S., & Chen, A., 1997, MNRAS, 287, 867

Kilkenny, D., Worters, H. L., O'Donoghue, D., Koen, C., Koen, T. Hambly, N. MacGillivray, H. & Stobie, R. S., 2016, MNRAS, 459, 4343

Koen, C., 1998, MNRAS, 300, 567

Kostov, V. B., Moore, K., Tamayo, D., Jayawardhana, R., & Rinehart, S. A. 2016, ApJ, 832, 183

Kupfer, T., Geier, S., Heber, U., et al. 2015, A&A, 576, A44

Lenz, P., 2004, Communications in Asteroseismology, 144

Lynas-Gray, A. E. 2013, in Astronomical Society of the Pacific Conference Series, Vol. 479, Progress in Physics of the Sun and Stars: A New Era in Helio- and Asteroseismology, ed. H. Shibahashi, & A. E. Lynas-Gray, 273

Lutz, R., 2011, Ph.D thesis, Georg-August-Universität

Mullally, Fergal, Winget, D. E., Degennaro, S., Jeffery, E., Thompson, S. E., Chandler, D., & Kepler, S. O., 2008, ApJ, 676, 573

Németh, P., Kawka, A., & Vennes, S. 2012, MNRAS, 427, 2180

O'Donoghue, D., Koen C., & Kilkenny D., 1996, MNRAS, 278, 1075

O'Donoghue, D., Lynas-Gray, A. E., Kilkenny, D., Stobie, R. S., & Koen, C., 1997, MNRAS, 285, 657

Oreiro, R., Ulla, A., Pérez Hernández, F., Østensen, R., Rodríguez López, C., & MacDonald, J., 2004, A&A, 418, 243.

Østensen, R., Solheim, J.-E., Heber, U., Silvotti, R., Dreizler, S., & Edelmann, H., 2001, A&A, 368, 175

Østensen, R., Oreiro, R., Solheim, J. -E., Heber, U., et al., 2010, A&A, 513, 6

Østensen, R. H., & Van Winckel, H. 2012, in Astronomical Society of the Pacific Conference Series, Vol. 452, Fifth Meeting on Hot Subdwarf Stars and Related Objects, ed. D. Kilkenny, C. S. Jeffery, & C. Koen, 163

Otani, T., 2015, Ph.D thesis, Florida Institute of Technology

Paparo, M., Szeidl, B., & Mahdy, H. A., 1988, Ap&SS, 149, 73

Paxton, B., Bildsten, L., Dotter, A., et al. 2011, ApJS, 192, 3

Paxton, B., Cantiello, M., Arras, P., et al. 2013, ApJS, 208, 4

Paxton, B., Marchant, P., Schwab, J., et al. 2015, ApJS, 220, 15

Press W. H., Teukolsky S. A., Vetterling W. T., Flannery B. P., 1992, Numerical Recipes (Cambridge: Cambridge Univ. Press), Chapter 15

Qian, S. B. et al., 2009, ApJ, 695, 163

Randall, S. K., Fontaine, G., Charpinet, S., Lynas-Gray, A. E., Lopes, I. P., O'Toole, S. J., & Brassard, P., 2006, ApJ, 648, 637

Randall, S. K., Van Grootel, V., Fontaine, G., Charpinet, S., & Brassard, P. 2009, A&A, 507, 911

Saffer, R. A., Bergeron, P., Koester, D., & Liebert, J., 1994, ApJ, 533, 984

Schechter, P. L., Mateo, M., & Saha, A., 1993, PASP, 105, 1342

Schmidt-Kaler, Th., 1982, $Landolt-BornsteinNewSeries$, Vol. 2b, Springer Verlan, New York

Schuh, S., Huber, J., Dreizler, S., Heber, U., O'Toole, S. J., Green, E. M., & Fontaine, G., 2006, A&A, 445, 31

Silvotti, R. et al., 2007, Nature, 449, 189

Silvotti, R., Szabó, R., Degroote, P., Østensen, R. H., & Schuh, S., 2011, AIP Conf. Proc., 1331, 133

Silvotti, R., Østensen, R., Telting, J., & Lovis, C., 2014, in Van Grootel, V., Green, E., Fontaine, G., & Charpinet, S., eds, ASP Conf. Ser., Vol. 481, 6th Meeting on Hot Subdwarf Stars and Related Objects., Astron. Soc. Pac., San Francisco, p. 13

Stobie, R. S. et al., 1997, MNRAS, 287, 848

Sullivan, D. J., Metcalfe, T. S., O'Donoghue, D., Winget, D. E., et al., 2008, MNRAS, 387, 137.

Tody, D., 1986, in D. L. Crawford, ed. Proc. SPIE Instrumentation in Astronomy VI, 627, 733

Tody, D., 1993, in eds. R.J. Hanisch, R. J. V. Brissenden, and J. Barnes, eds. ASP Conf. Ser., Vol. 52, Astronomical Data Analysis Software and System II, 173

Veras, D., Georgakarakos, N., Dobbs-Dixon, I., & Gänsicke, B. T. 2017, MNRAS, 465, 2053

Vos, J., Østensen, R. H., Marchant, P., & Van Winckel, H. 2015, A&A, 579, A49

Vos, J., Németh, P. Vučković, M., Østensen, R. & Parsons, S., 2017, MNRAS, 473, 693

Völschow, M., Schleicher, D. R. G., Perdelwitz, V., & Banerjee, R. 2016, A&A, 587, A34

Wade R., Barlow, B., Liss. S., & Stark, M. 2014, in Van Grootel, V., Green, E., Fontaine, G., & Charpinet, S., eds, ASP Conf. Ser., Vol. 481, 6th Meeting on Hot Subdwarf Stars and Related Objects. Astron. Soc. Pac., San Francisco, p. 311

Winget, D. E., & Kepler, S. O., 2008, ARA&A, 46, 157

Xiong, H., Chen, X., Podsiadlowski, P., Li, Y., & Han, Z. 2017, A&A, 599, A54

Zorotovic, M., & Schreiber, M. R. 2013, A&A, 549, A95